

300W CHARGER DESIGN UTILIZING FANLESS LLC CONVERTER FOR LEAD-ACID BATTERY CHARGING APPLICATIONS

Khanh Duc NGUYEN

*School of Electrical and Electronic
Engineering, Hanoi University of
Science and Technology
Hanoi, Vietnam*
khanh.nd202415@sis.hust.edu.vn

Van Thai MAI

*School of Electrical and Electronic
Engineering, Hanoi University of
Science and Technology
Hanoi, Vietnam*
thai.mv202698@sis.hust.edu.vn

Quang Huy NGUYEN

*School of Electrical and Electronic
Engineering, Hanoi University of
Science and Technology
Hanoi, Vietnam*
huy.nq181528@sis.hust.edu.vn

Duy Dinh NGUYEN

*School of Electrical and Electronic
Engineering, Hanoi University of
Science and Technology
Hanoi, Vietnam*
dinh.nguyenduy@sis.hust.edu.vn

ABSTRACT

This paper presents the design of a 300W charger for lead-acid battery charging applications. It focuses on achieving higher efficiency, increased power and component density, and cost-effectiveness. Resonant converters, particularly those using the LLC half-bridge configuration, are emphasized for their ability to operate at higher switching frequencies while minimizing losses. The charger's unique feature is its fanless design, ensuring compliance with EN60335-1 standards regarding temperature limits on the charger's surface. The paper presents the charger design, resolves surface temperature issues, and shares experimental results demonstrating its performance and temperature control during the lead-acid battery charging process.

Keywords: *LLC resonant converter, fanless, lead-acid battery, surface temperature.*

1. INTRODUCTION

The increasing need for battery-powered electric vehicles to reduce air pollution and replace fossil fuels has grown steadily over the past century [1]. Secondary batteries are crucial for EVs as they are extensively used to store renewable energy. In this context,

chargers play a vital role in enhancing battery performance and lifespan.

In this specific application, we introduce a 300W charger designed to operate within a 60-72V voltage range, primarily for charging lead-acid batteries in conventional electric motorcycles.

We've chosen the LLC resonant converter topology due to its benefits, including high efficiency, reduced switching losses by achieving zero voltage switching (ZVS), minimized electromagnetic interference (EMI), and high-power density [3]. This charger employs a fanless design with a plastic casing to enhance mechanical reliability by preventing dust and moisture ingress, eliminating noise and vibrations during operation. It's important to note that the absence of a fan may require a larger surface area for heat dissipation, potentially increasing the overall charger volume [5]

Complying with the EN60335-1 standard, which mandates a maximum allowable surface temperature of 75°C for the plastic casing, poses a challenge in the design of this high-power charger when using passive cooling methods. This article presents the charger's design and thermal design to achieve effective cooling in a fanless application. Finally, experimental results, including performance and temperature data on the charger's surfaces during operation, are provided.

2. HALF-BRIDGE LLC RESONANT CONVERTER DESIGN

2.1 Overview of the Charging System.

The proposed charging system is shown in Figure 1, consisting of an input EMI filter, a rectifier bridge, an isolated DC-DC converter, and the battery.

According to the IEC61000-3-2 standard, the power factor (PF) should not drop below 0.9 when the output power reaches 300W. However, for the purpose of cost savings, and as this specific application does not necessitate strict adherence to standards, a diode bridge is directly connected to the back of the LLC converter instead of implementing Power Factor Correction (PFC). In order to satisfy the 300W power requirement, a decision was made to employ a Half-bridge LLC resonant converter, with the goal of optimizing component count and reducing construction costs [4].

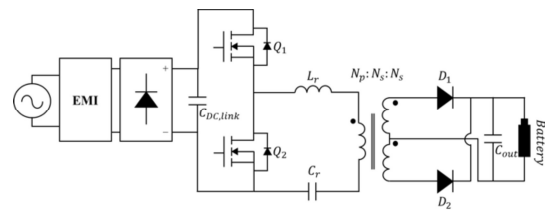


Fig. 1. Proposed Charger System

2.2 System Charging Design Specifications.

System requirements and design parameters of magnetizing inductance, resonant inductance and resonant capacitor values are given in Table I. Resonant frequency value is selected at 200kHz to minimize core loss and reduces EMI problems [3]. The magnetization inductance value is selected to achieve ZVS soft switching for the converter.

2.3 Components and Losses in the Charging System Design.

The losses of each charger component are calculated and simulated at the 300W operating point. It is evident that the most significant losses are associated with semiconductor components. Losses in semiconductor components account for 67.77% of the total charger losses. To reduce losses in

semiconductor components, one can enhance the characteristics of the components, such as reducing the conduction resistance of MOSFET ($R_{ds,on}$), reducing the switching time of MOSFET, or the forward voltage of rectifier diodes... Component selection is based on the available characteristics of components listed in Table II.

TABLE I. DESIGN SPECIFICATIONS

DESIGN PRAMETERS OF THE POSPOSED CHARGER			
<i>Parameter</i>	<i>Variable</i>	<i>Value</i>	<i>Unit</i>
Input Voltage Range	$V_{in}^{min} - V_{in}^{max}$	165 – 265	<i>Vrms</i>
Nominal Input Voltage	V_{in}^{nom}	220	<i>Vrms</i>
Output Voltage Range	$V_{out}^{min} - V_{out}^{max}$	60 – 72	<i>Vdc</i>
Nominal Output Voltage	V_{out}^{nom}	66.7	<i>Vdc</i>
Resonant Frequency	f_r	200	<i>kHz</i>
Switching Frequency	$f_{sw}^{min} - f_{sw}^{max}$	135 – 380	<i>kHz</i>
Transformers Turns Ratio	n	2.333	
Magnitizing Inductor	L_m	72.03	μH
Resonant Inductor	L_r	24.02	μH
Resonant Capacitor	C_r	26.4	<i>nC</i>
Charger size	$w \times l \times h$	98 × 161.8 × 30	<i>mm</i>
Surface temperature max	T_{max}	75	$^{\circ}C$

TABLE II. CHARGER COMPONENTS AND LOSSES

COMPONENTS			
<i>Name</i>	<i>Value</i>	<i>Number</i>	<i>Loss</i>
MOSFET	IPA60R120P7	2	5.336 [W]
Diode Bridge	GBU2510	1	3.502 [W]
Output rectifier	MBR40200CT	1	2.3 [W]
Transformer		1	4.78 [W]
Resonant Inductor		1	0.52 [W]

3. THERMAL DESIGN FOR CHARGING SYSTEM

3.1 The goals of thermal design.

The battery charger's thermal design has two goals:

3.1.1) Adequate heat dissipation for parts, particularly for power semiconductors, to maintain performance and dependability.

3.1.2) Adherence to surface temperature standards to avoid handling-related fires and burns.

According to European standard EN 60335-1, the maximum allowable surface temperature of plastic housing is 75 °C. Therefore, for this battery charger, a maximum temperature on the plastic case of $T_{s,max} = 65^{\circ}\text{C}$ is selected with an ambient temperature of $T_{amb} = 30^{\circ}\text{C}$.

3.2 Cooling methods.

The article uses a fanless structure along with a plastic case for the charger, so the primary heat dissipation method

used is natural convection on the case surface. Since air is inferior in conducting heat (the thermal conductivity of air is only 0.0261 W/m.K), the charger is filled with an epoxy compound with higher thermal conductivity (from 0.6 to 1 W/m.K). In addition to improved heat transfer, these materials provide excellent mechanical and electrical protection for the device. Aluminum heatsinks are also used to increase the efficiency of heat transfer to the case surface for large heat sources. The detailed structure and dimensions of the heatsink are shown in Fig.1. With the charger loss Q , the case surface area where convection occurs A_s , and the convection heat transfer coefficient h , the average temperature on the case surface $T_{s,avg}$ is calculated using the following formula:

$$T_{s,avg} = \frac{Q}{hA_s} + T_{amb}$$

The average convective heat transfer coefficient on the surface of the case is determined experimentally with $h = 17 \text{ W/m}^2\cdot\text{K}$. With the case size as shown in Figure 1, the surface area where natural convection occurs $A_s = 368 \text{ cm}^2$, the average temperature on the case surface $T_{s,avg} = 56.3^\circ\text{C}$. ANSYS Electronics Desktop thermal simulation software was used to create model (see Fig. 2) and verify theoretical calculations. The results show the average temperature on the case surface $T_{s,avg} = 59^\circ\text{C}$ (see Fig.3).

Compared to the structure without using epoxy, because the area where natural convection occurs is reduced, the average temperature on the case surface theoretically increases to $T_{s,avg} = 72.6^\circ\text{C}$. Verified with simulation, the temperature at hotspot (see Fig.3) increases to $T_{s,max} = 76.1^\circ\text{C}$. From there, it shows that the temperature rise has decreased by 38.3% and 37.1% respectively in calculation and simulation when using epoxy structure.

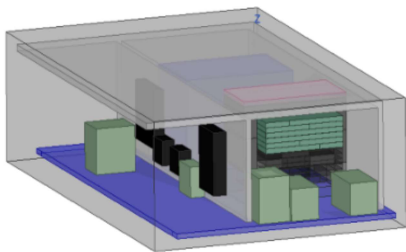


Fig. 2. Simulation model uses ANSYS Electronics Desktop

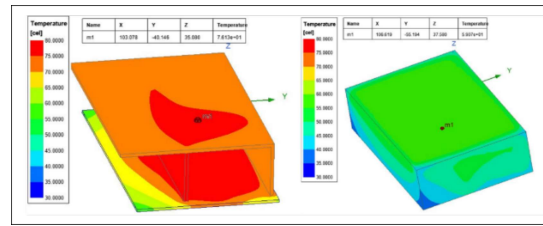


Fig. 3. Temperature Distribution on the Surface in Simulation. The left image is the charger without epoxy, and the right image is the epoxy-filled charger.

4. EXPERIMENTAL RESULT

The charger is designed based on the figures given in Table I. An image of the charger is given in Fig.4. Current and voltage waveform tests on low-side MOSFET Q2 at voltage $V_{in} = 220\text{V}_{rms}$ and $V_{out} = 72\text{V}$ are shown in Fig.5.

Fig.5 demonstrates that there are no voltage and current spikes on the low-side switch (MOSFET Q2). Due to the utilization of CoolMOS P7 current valve from Infineon, there is an occurrence of Early channel shutdown when turning off the MOSFET. This phenomenon results in reduced switching losses of the MOSFET.

The temperature measurements were taken at an average ambient temperature of 30°C using a UNI-T infrared thermometer. The thermal measurement points, as illustrated in Fig.6, include Point 1 - Along the side adjacent to the long heatsink, Point 2 - Near the transformer on the upper edge, Point 3 - Along the side not adjacent to the long heatsink, Point 4 - At the top of

the input, and Point 5 - The transformer machine placement point.

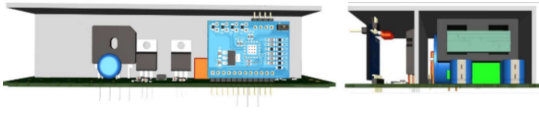


Fig. 4. The PCB Layout of the charger

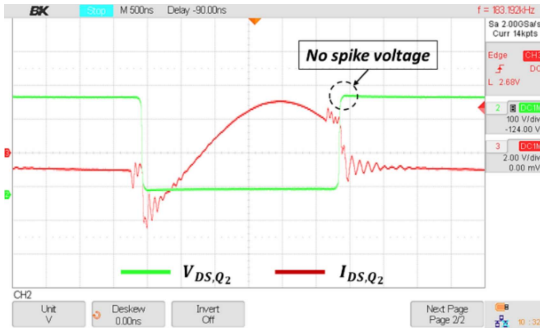


Fig. 5. Current and voltage waveforms on low-side MOSFET Q2 at voltage $V_{in} = 220V_{rms}$ and $V_{out} = 72V$.

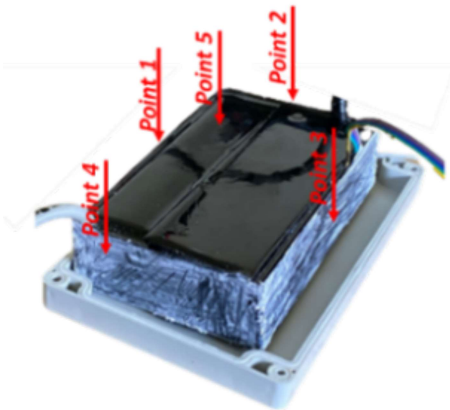


Fig. 6. The experiment measured the surface temperature when the charger was filled with epoxy.

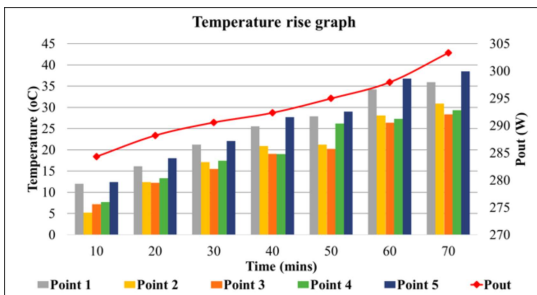


Fig. 7. Graph of temperature increase on epoxy-filled charger surface.

In Fig.7, you can observe temperature measurements at an output power of 300W and an ambient temperature of 30°C. The temperatures between surfaces 2, 3, and 4 are relatively uniform. However, the two surfaces 1 and 5, which have a larger contact area with the heat sink, are approximately 5°C hotter than the other surfaces. The hottest point is the direct interface between the transformer and the heat sink, where the temperature rises to 38°C. This means that the surface temperature reaches 68°C at rated power. The achieved temperature levels meet the design requirements and comply with the EN60335-1 standard.

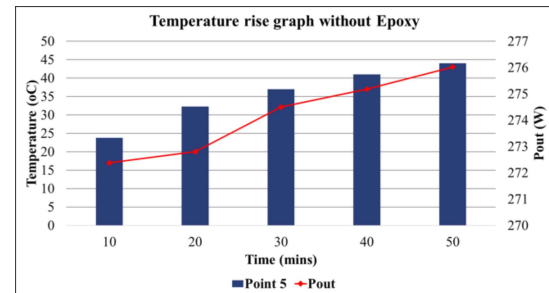


Fig. 8. Temperature increase graph on charger surface without epoxy.

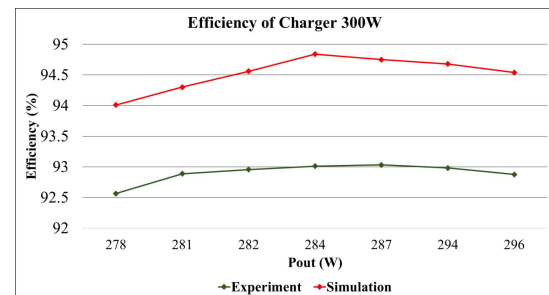


Fig. 9. Charging Efficiency Discrepancy: Experimental vs. Simulated Graph

The highest temperature on the charger without epoxy encapsulation is presented in Fig.8, with a hotspot occurring at a power level of 276W, and a measurement time of 50 minutes. The maximum temperature increases reached 44°C, exceeding the allowable limit, prompting the experiment to be halted. It is evident that the temperature increases at 50 minutes when using epoxy with a higher power level is 27.7°C, which is a 37% reduction compared to the experiment without epoxy. This aligns entirely with the calculations and simulations discussed above.

Fig.9 illustrates the charger's performance in both experimental and simulated scenarios. The experimental performance results show a slight deviation, lower by 0.8% (2.4W), compared to the simulated outcome. This discrepancy suggests that the simulation model is still lacking in terms of loss estimation accuracy. However, it can also be explained by the additional 7°C increase in surface temperature relative to the simulation and calculation.

CONCLUSION

This article describes the design of a 300W fanless charger specifically developed for charging lead-acid batteries in small and medium-sized electric vehicles. Emphasizing the critical role of temperature control in this application, the study introduces a novel approach using epoxy as a heat-conductive material to ensure uniform heat distribution across the charger's surface. This method aims to reduce the temperature at the highest point on the surface while simultaneously increasing the convective surface area with air, thereby improving heat dissipation efficiency. Experimental results demonstrate a maximum recorded temperature of 68°C, meeting the requirements outlined in the EN60335-1 standard. Additionally, the findings highlight epoxy's ability to improve temperature control by 37% in this application.

REFERENCES

- [1] IEA (2022), Global EV Outlook 2022, IEA, Paris <https://www.iea.org/reports/global-ev-outlook-2022>, License: CC BY 4.0.
- [2] Keshan, Hardik, Jesse Thornburg, and Taha Selim Ustun. "Comparison of lead-acid and lithium ion batteries for stationary storage in off-grid energy systems." (2016): 30-7.
- [3] Huang, Hong. "Designing an LLC resonant half-bridge power converter." 2010 Texas Instruments Power Supply Design Seminar, SEM1900, Topic. Vol. 3. Dallas, TX, USA: Texas Instruments Incorporated, 2010.
- [4] Zeng, Junming, et al. "LLC resonant converter topologies and industrial applications—A review." *Chinese Journal of Electrical Engineering* 6.3 (2020): 73-84.
- [5] Ahmed, Tousif. "Fanless Cooling Using Thermal Energy Storage Materials: Phase Change Materials (PCM) Encapsulated in."